

Organic & Biomolecular Chemistry

Accepted Manuscript



This is an *Accepted Manuscript*, which has been through the Royal Society of Chemistry peer review process and has been accepted for publication.

Accepted Manuscripts are published online shortly after acceptance, before technical editing, formatting and proof reading. Using this free service, authors can make their results available to the community, in citable form, before we publish the edited article. We will replace this *Accepted Manuscript* with the edited and formatted *Advance Article* as soon as it is available.

You can find more information about *Accepted Manuscripts* in the [Information for Authors](#).

Please note that technical editing may introduce minor changes to the text and/or graphics, which may alter content. The journal's standard [Terms & Conditions](#) and the [Ethical guidelines](#) still apply. In no event shall the Royal Society of Chemistry be held responsible for any errors or omissions in this *Accepted Manuscript* or any consequences arising from the use of any information it contains.

Understanding the Domino Reaction between 3-Chloroindoles and Methyl Coumalate yielding Carbazoles. A DFT Study

Luis R. Domingo,^{*a} José A. Sáez^b and Saeed R. Emamian^c

^a *Departamento de Química Orgánica, Universidad de Valencia, Dr. Moliner 50, E-46100 Burjassot, Valencia, Spain.*

^b *Instituto de Tecnología Química UPV-CSIC, Camino de Vera s/n, 46022 Valencia, Spain.*

^c *Chemistry Department, Shahrood Branch, Islamic Azad University, Shahrood, Iran.*

E-mail: domingo@utopia.uv.es

Web: www.luisrdomingo.com

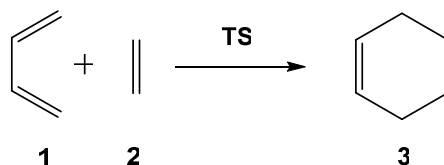
Abstract

The molecular mechanism of the reaction between *N*-methyl-3-chloroindole and methyl coumalate yielding carbazole has been studied using DFT methods at the MPWB1K/6-311G(d,p) level in toluene. This reaction is a domino process that comprises three consecutive reactions: *i*) a polar Diels-Alder (P-DA) reaction between indole and methyl coumalate yielding two stereoisomeric [2+4] cycloadducts (CAs); *ii*) an elimination of HCl from these CAs affording two stereoisomeric intermediates; and *iii*) an extrusion of CO₂ in these intermediates, finally yielding the carbazole. This P-DA reaction presents a complete regioselective and slightly *exo* selective fashion. In spite of the high polar character of this P-DA reaction, it presents a high activation enthalpy of 21.8 kcal/mol due to the loss of the aromatic character of the indole along the C–C bond formation. Thermodynamic calculations suggest that the P-DA reaction is the rate-determining step of this domino reaction; in addition, the initial HCl elimination in the formal [2+4] CAs is kinetically favoured over the extrusion of CO₂. Although the P-DA reaction is kinetically and thermodynamically very unfavourable, the easier HCl and CO₂ elimination from the [2+4] CAs together with the strong exergonic character of the CO₂ extrusion makes the P-DA reaction irreversible. ELF topological analysis of the bonding changes along the P-DA reaction supports a *two-stage one-step* mechanism. Analysis of the global DFT reactivity indices at the ground state of the reagents confirms the high polar character of this P-DA reaction. Finally, the complete regioselectivity of the studied reactions can be explained using the Parr functions.

Introduction

The Diels-Alder (DA) reaction is arguably one of the most powerful reactions in the arsenal of the synthetic organic chemist.¹ It permits the rapid construction of six-membered carbocycles from a 1,3-butadiene, the diene, and an ethylene derivative, the dienophile, with a high stereo- and regioselectivity. The diversity of substitution which may be present in the diene and the dienophile makes the DA reaction one of the most important synthetic organic reactions.

The simplest DA reaction between butadiene **1** and ethylene **2** is generally presented in all textbooks as the prototype of this cycloaddition type, but this reaction cannot easily be carried out experimentally due to its unfavourable activation energy, 27.5 kcal/mol (see Scheme 1).²



Scheme 1. DA reaction between butadiene **1** and ethylene **2**.

An exhaustive study of DA reactions established a very good correlation between the experimental reaction rates and the global electron density transfer (GEDT) computed at the transition state structures (TSs) of the reactions. This finding allowed us to propose the polar Diels-Alder (P-DA) reaction mechanism³ which is characterised by the favourable nucleophilic/electrophilic interactions at the corresponding TSs. There are only very few DA reactions, namely non-polar Diels-Alder reactions (N-DA), which do not follow the polar mechanism. However, N-DA reactions, which are characterised by a very low GEDT at the TSs, have a low synthetic interest due to the drastic reaction conditions required for the reaction to take place.

Thus, while N-DA reactions have little synthetic interest as they demand harsh reaction conditions, the feasibility of a P-DA reaction increases with the polar character of the reaction, *i.e.* the electrophilic/nucleophilic character of the reagents is the driving force in P-DA reactions. These behaviours can easily be anticipated by analysing the

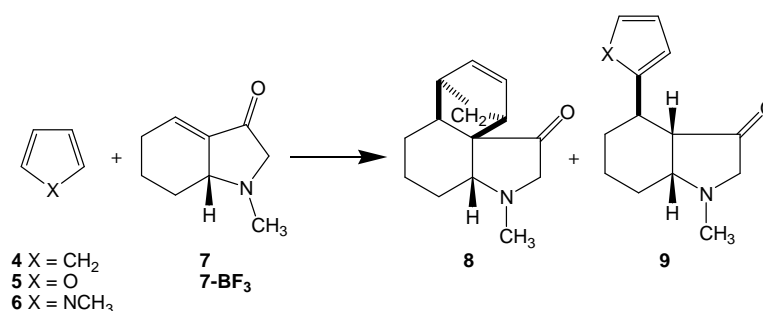
4

electrophilicity ω index⁴ and the nucleophilicity N index,⁵ defined within the conceptual density functional theory (DFT),⁶ at the ground state of the reagents.

DA reactions involving aromatic heterocyclic compounds (AHCs) constitute a cornerstone for the construction of polycyclic heterocyclic compounds.¹ Five-membered aromatic heterocyclic compounds (FAHCs), such as furans, pyrroles, and others are important reagents that participate in P-DA reactions either as the diene or dienophile. While single FAHCs, due to their nucleophilic nature, can participate as the diene in P-DA reactions toward electrophilically activated dienophiles, they do not readily participate as a dienophile, demanding a strong chemical activation for such a reaction. Presence of strong electron-withdrawing groups (EWGs), such as the nitro (NO₂) one, electrophilically activates FAHCs participating in P-DA reactions as the dienophile.⁷ On the other hand, substituted indoles, benzofurans, and benzothiophenes bearing a strong EWG such as nitro, have been used as the dienophile in P-DA reactions.⁸

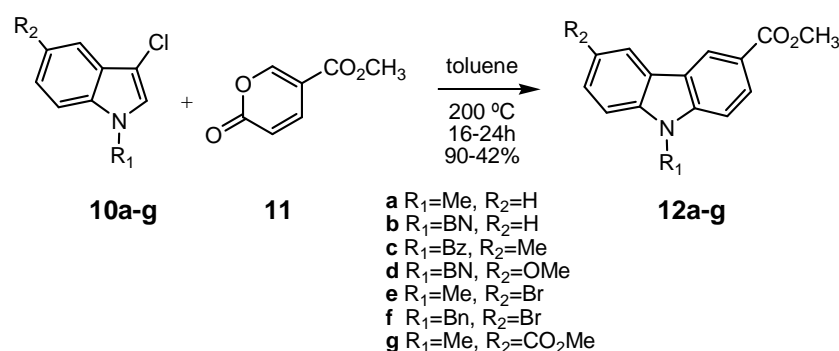
The participation of FAHCs in DA reactions widely has been studied using theoretical methods.⁹ Recently, the P-DA reactions of bicyclic enone **7** with Cp **4**, furan **5** and *N*-methyl pyrrole **6** have been theoretically studied (see Scheme 2).¹⁰ No reaction takes place in the absence of Lewis acid (LA) catalysts as a consequence of the high activation energy associated with these reactions, 19.1 (**4**), 26.2 (**5**), and 29.9 (**6**) kcal/mol. *N*-methyl pyrrole **6** displays a larger nucleophilic character, $N = 3.70$ eV,⁵ than Cp **4**, $N = 3.36$ eV. Nevertheless, the P-DA reaction of *N*-methyl pyrrole **6** presented a higher activation energy. Electrophilic activation of enone **7**, $\omega = 1.47$ eV,⁴ by formation of a complex with BF₃ LA (**7-BF₃**), $\omega = 2.89$ eV, and inclusion of solvent effects clearly favour the reactions, the activation energies being 9.2 (**4**), 11.0 (**5**), and 6.4 (**6**) kcal/mol. However, a different reactivity was displayed by Cp **4** vs FAHCs **5** and **6**. Thus, while the reaction of complex **7-BF₃** with Cp **4** generates the expected *exo* [2+4] cycloadduct (CA) **8** via a *two-stage one-step* mechanism,¹¹ the reactions with FAHCs **5** and **6** produce the Michael adduct **9** via a stepwise mechanism with formation of zwitterionic intermediates. These reactions were characterised by the initial nucleophilic/electrophilic two-center interaction between the most nucleophilic centers of these dienes and the most electrophilic center of complex **7-BF₃**. The aforementioned studies imply a different reactivity between Cp **4** and the FAHCs **5** and **6**, related to the

aromatic character of the FAHCs, which is lost along the nucleophilic attack. This behaviour has two important consequences: i) the activation energies associated with P-DA reactions involving FAHCs are higher than those involving conjugated dienes; and ii) a competitive aromatic electrophilic substitution (AES) reaction can take place if the reaction involves strong nucleophilic FAHCs.



Scheme 2

Very recently, Kraus has experimentally studied the reaction of *N*-methyl-3-chloroindoles **10a-g** with methyl coumalate **11** yielding carbazoles **12a-g** (see Scheme 3).¹² Formation of carbazoles **12a-g** is a domino reaction that begins with the P-DA reaction between 3-chloroindoles **10a-g** and methyl coumalate **11** to yield the corresponding formal [2+4] CAs, which undergo a rapid CO₂ and HCl elimination yielding carbazoles **12a-g**. In spite of the polar character of these DA reactions, they require drastic reaction conditions, 200 °C and 16-24 h, indicating that the reactions are not favoured.



Scheme 3. Some of Kraus's domino reactions of *N*-methyl-3-chloroindole **10a-g** with methyl coumalate **11**.

Herein, a DFT study of the domino reaction of 3-chloroindole **10a** with methyl coumalate **11** yielding carbazole **12a**, experimentally reported by Kraus,¹² is studied at the MPWB1K/6-311G(d,p) level in toluene in order to characterise the reaction mechanism of these domino processes as well as the participation of nucleophilic 3-chloroindoles **10a-g** in P-DA reactions. An electron localisation function¹³ (ELF) topological analysis of the most relevant points along the intrinsic reaction coordinate¹⁴ (IRC) curve of the P-DA reaction between **10a** and **11** is performed in order to characterise the bonding changes along the cycloaddition reaction, and thus to establish the molecular mechanism of this P-DA reaction.¹⁵

Computational Methods

DFT computations were carried out using the MPWB1K¹⁶ exchange-correlation functional, together with the standard 6-311G(d,p) basis set.¹⁷ Optimisations were performed using Berni's analytical gradient optimisation method.¹⁸ The stationary points were characterised by frequency computations in order to verify that TSs have one and only one imaginary frequency. The IRC paths¹⁴ were traced in order to check the energy profiles connecting each TS to the two associated minima of the proposed mechanism using the second order González-Schlegel integration method.¹⁹ Solvent effects of toluene ($\epsilon = 2.37$) in the optimisations were taken into account using the polarisable continuum model (PCM) as developed by Tomasi's group²⁰ in the framework of the self-consistent reaction field (SCRF).²¹ It is worth to note that only the reaction with **10a** was performed in acetonitrile, while the other domino reactions between *N*-methyl-3-chloroindoles **10b-g** and methyl coumalate **11** were carried out in toluene (see Scheme 3). Consequently, in the present study, we also chosen toluene as solvent. Values of enthalpies, entropies, and Gibbs free energies in toluene were calculated with standard statistical thermodynamics at 200 °C and 1 atm.¹⁷ The electronic structures of stationary points were analysed by the natural bond orbital (NBO) method²² and ELF topological analysis, $\eta(\mathbf{r})$.²³ The ELF study was performed with the TopMod program²⁴ using the corresponding monodeterminantal wavefunctions of the selected structures of the IRC. All computations were carried out with the Gaussian 09 suite of programs.²⁵

The global electrophilicity index,⁴ ω , is given by the following expression, $\omega = (\mu^2 / 2\eta)$, based on the electronic chemical potential μ and the chemical hardness η . Both quantities may be approached in terms of the one-electron energies of the frontier molecular orbitals HOMO and LUMO, ϵ_H and ϵ_L , as $\mu \approx (\epsilon_H + \epsilon_L) / 2$ and $\eta \approx (\epsilon_L - \epsilon_H)$, respectively.²⁶ The global nucleophilicity index,⁵ N , based on the HOMO energies obtained within the Kohn-Sham scheme,²⁷ is defined as $N = E_{\text{HOMO}}(\text{Nu}) - E_{\text{HOMO}}(\text{TCE})$. This relative nucleophilicity index refers to tetracyanoethylene (TCE). Electrophilic P_k^+ and nucleophilic P_k^- Parr functions²⁸ were obtained through the analysis of the Mulliken atomic spin density (ASD) of the radical anion of methyl coumalate **11** and the radical cation of 3-chloroindole **10a**, respectively.

Results and discussion

The present study is divided into three parts: i) first, the reaction paths involved in the domino reaction of 3-chloroindole **10a** with methyl coumalate **11** yielding carbazole **12a** is studied; ii) in the second part, an ELF topological analysis along the P-DA between 3-chloroindole **10a** and methyl coumalate **11** is carried out in order to characterise the molecular mechanism; and iii) finally, an analysis of the DFT reactivity indices of the reagents involved in this domino reaction is performed.

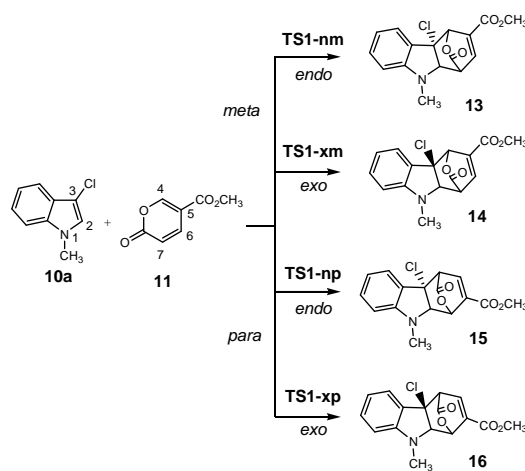
i) Study of the reaction paths involved in the domino reaction of 3-chloroindole 10a with methyl coumalate 11.

The reaction of 3-chloroindole **10a** with methyl coumalate **11** yielding carbazole **12a** is a domino process that comprises three consecutive reactions (see Scheme 4): *i*) a P-DA reaction between 3-chloroindole **10a** and methyl coumalate **11** to yield the corresponding formal [2+4] CAs **13** and **14**; *ii*) an extrusion of CO₂ in these CAs affording the corresponding intermediates; and finally *iii*) an elimination of hydrochloric acid to give carbazole **12a**. Alternatively, CAs **13** and **14** can undergo a competitive hydrochloric acid elimination yielding the corresponding intermediates which in turn experience a further extrusion of CO₂ giving carbazole **12a**. The MPWB1K/6-311G(d,p) relative enthalpies, entropies, and Gibbs free energies in toluene

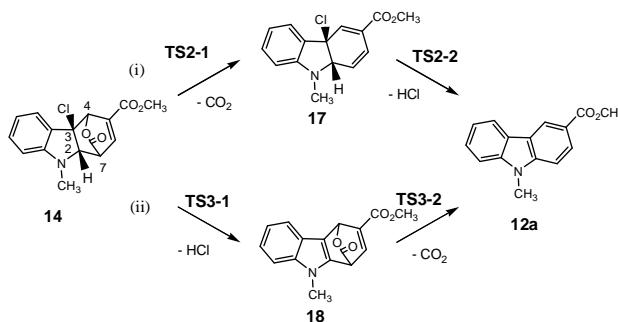
for the stationary points involved in this domino reaction are given in Table 1, while enthalpies, entropies, and Gibbs free energies in toluene are given in the Supporting Information.

Due to the asymmetry of both reagents, four competitive channels are feasible for the P-DA reaction between 3-chloroindole **10a** and methyl coumalate **11**. They are related to the two stereoisomeric approach modes of the methyl carboxylate of **11** relative to the aromatic ring of indole **10a**, named *endo* and *exo*, and the two regioisomeric approach modes of the C3 carbon of 3-chloroindole **10a** toward the C4 or C7 carbons of methyl coumalate **11**; depending on the position of the chlorine atom relative to the methyl carboxylate, the two regioisomeric possibilities are named *meta* and *para*. P-DA reactions are completely regioselective. Thus, an analysis of the Parr functions²⁸ allows ruling out the stereoisomeric paths associated with the nucleophilic attack of the C3 carbon of 3-chloroindole **10a** on the C7 carbon of methyl coumalate **11** (see below). Consequently, only the *meta* regioisomeric channels were studied.

a) P-DA reaction between 3-chloroindole **10a** and methyl coumalate **11**.



b) competitive paths associated with the elimination of CO₂ and HCl.



Scheme 4. Reaction paths involved in the domino reaction between 3-chloroindole **10a** and methyl coumalate **11**.

Table 1. MPWB1K/6-311G(d,p) relative^a enthalpies (ΔH , in kcal/mol), entropies (ΔS , in cal/molK), and Gibbs free energies (ΔG , in kcal/mol), computed at 200 °C and 1 atm in toluene, for species involved in the domino reaction between 3-chloroindole **10a** and methyl coumalate **11**.

	ΔH	ΔS	ΔG
TS1-nm	23.0	-49.5	46.4
TS1-xm	21.8	-47.4	44.3
13	-11.5	-49.8	12.1
14	-10.8	-50.1	13.0
TS2-1	27.7	-46.6	49.8
17	-11.9	-6.2	-8.9
TS2-2	1.1	-1.3	1.7
TS3-1	20.4	-47.9	43.0
18	-3.9	-10.8	1.2
TS3-2	9.5	-10.9	14.7
12a	-53.3	30.4	-67.7

a: relative to 10a+11.

An analysis of the stationary points involved in the two stereoisomeric paths indicates that this P-DA reaction takes place through a one-step mechanism. Consequently, two TSs, **TS1-nm** and **TS1-xm**, and the corresponding formal [2+4] CAs **13** and **14** were located and characterised. Along the *meta* channels, the activation enthalpies in toluene associated with the nucleophilic attack of the C3 carbon of 3-chloroindole **10a** on the C4 carbon of methyl coumalate **11** are 23.0 (**TS1-nm**) and 21.8 (**TS1-xm**) kcal/mol; the reaction being slightly *exo* selective. Formation of the corresponding formal [2+4] CAs is exothermic; -11.5 (**13**) and -10.8 (**14**) kcal/mol.

Since both CAs **13** and **14** yield carbazole **12a** after CO₂ and HCl extrusion, only the reaction paths associated with the conversion of the formal *exo* [2+4] CA **14** into carbazole **12a** were analysed. Two competitive channels are feasible for the conversion of **14** into carbazole **12a** (see Scheme 4). Along channel (i) extrusion of CO₂ from **14** via **TS2-1** yields intermediate **17** which by a subsequent HCl elimination via **TS2-2** affords carbazole **12a**. Along channel (ii), HCl elimination from **14** via **TS3-1** yields intermediate **18** which by extrusion of CO₂ via **TS3-2** yields carbazole **12a**. Along the two competitive channels, both the extrusion of CO₂ and the elimination of HCl take

place *via* a one-step mechanism. Consequently, only one TS was found for each one of these reactions.

Along channel (i) the activation enthalpy associated with the extrusion of CO₂ *via* **TS2-1** is 38.5 kcal/mol; formation of intermediate **17** is slightly endothermic by 1.1 kcal/mol. The activation enthalpy associated with the subsequent HCl elimination is 13.0 kcal/mol; formation of carbazole **12a** is exothermic by 41.4 kcal/mol. If the overall domino reaction is considered, formation of carbazole **12a** along this domino process is strongly exothermic; -53.3 kcal/mol.

Along channel (ii), the activation enthalpy associated with the initial elimination of HCl *via* **TS3-1** is 31.2 kcal/mol; formation of intermediate **18** is endothermic by 6.9 kcal/mol. From this intermediate, the activation enthalpy associated with the subsequent extrusion of CO₂ *via* **TS3-2** is 13.4 kcal/mol; formation of carbazole **12a** is exothermic by 49.4 kcal/mol.

When the relative enthalpies of the two competitive channels for the formation of carbazole **12a** are compared, it turns out that extrusion of CO₂ *via* **TS2-1** from CA **14** is 7.3 kcal/mol more energetic than the elimination of HCl *via* **TS3-1**. In addition, extrusion of CO₂ from CA **14** is 25.1 kcal/mol more unfavourable than the extrusion from intermediate **18**. These energy results make it possible to clearly rule out formation of carbazole **12a** *via* channel (i).

When including entropies with enthalpies, different results of activation Gibbs free energies of the reactions involved in this domino reaction are produced. While the activation Gibbs free energies associated with the P-DA reaction significantly increase due to the bimolecular nature of the reaction, those associated with HCl and CO₂ extrusions slightly decrease due to their unimolecular nature.

The schematic representation of the relative Gibbs free energy profile for the domino reaction between 3-chloroindole **10a** and methyl coumalate **11** is given in Figure 1. As can be seen, **TS3-2** and **TS3-3** are located below **TS1-xm**; consequently the first P-DA reaction of this domino process is the rate-determining step of the reaction.

Although the P-DA reaction between 3-chloroindole **10a** and methyl coumalate **11** is exothermic by *ca.* 11 kcal/mol, the bimolecular nature of the reaction together with the high temperature at which the reaction is carried out, 200 °C, makes the reaction

endergonic by 12-13 kcal/mol. Consequently, this P-DA reaction is kinetically and thermodynamically very unfavourable. However, the low activation enthalpies found for the HCl and CO₂ elimination together with the strong exergonic character of the CO₂ extrusion makes the overall domino process irreversible.

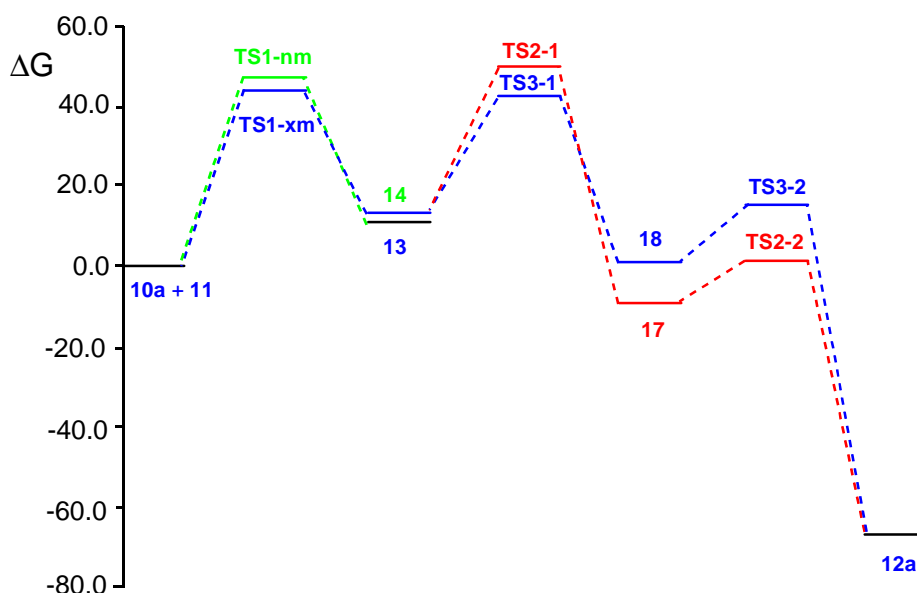


Figure 1. Relative Gibbs free energy profile, in kcal/mol, for the domino reaction between 3-chloroindole **10a** and methyl coumalate **11** in toluene.

The optimised geometries of the TSs involved in the domino reaction between 3-chloroindole **10a** and methyl coumalate **11** are given in Figure 2. In gas phase, at the TSs associated with the P-DA reaction between 3-chloroindole **10a** and methyl coumalate **11**, the lengths of C3–C4 and C2–C6 forming bonds are 1.750 and 2.704 Å at **TS1-nm**, and 1.863 and 2.779 Å at **TS1-xm**, respectively. These lengths allow establishing two appealing conclusions: i) the great difference between these distances, $\Delta d > 0.9$, allows establishing that this P-DA reaction will take place through a *two-stage one-step* mechanism¹¹ characterised by the nucleophilic attack of the C3 carbon of chloroindole **10a** on the C4 carbon of methyl coumalate **11**; and ii) the short distance between the C3 and C4 carbons at both TSs, $d(\text{C3–C4})$ around 1.8 Å, indicates that the formation of the C3–C4 single bond has begun at these TSs (see later).²⁹

At the TSs associated with the extrusion of CO₂, the lengths between the atoms involved in the C–C and C–O breaking bonds are 1.819 and 2.089 Å at **TS2-1** and

12

1.716 and 2.560 Å at **TS3-2**, respectively. These lengths indicate that the C–O breaking bond is more advanced than the C–C one. In addition, at the most favourable **TS3-2** while the C–O breaking bond is more advanced than at **TS2-1**, the C–C breaking bond is slightly more delayed; that is, the more asynchronous **TS3-2**, the more favourable it is.

Finally, at the TSs associated with the HCl elimination, the lengths between the atoms involved in the C–Cl and C–H breaking bonds are 2.666 and 1.123 Å at **TS2-2**, and 2.965 and 1.136 Å at **TS3-1**, respectively. These lengths indicate that while the C–Cl breaking bond is very advanced, the C–H breaking bond is much delayed.

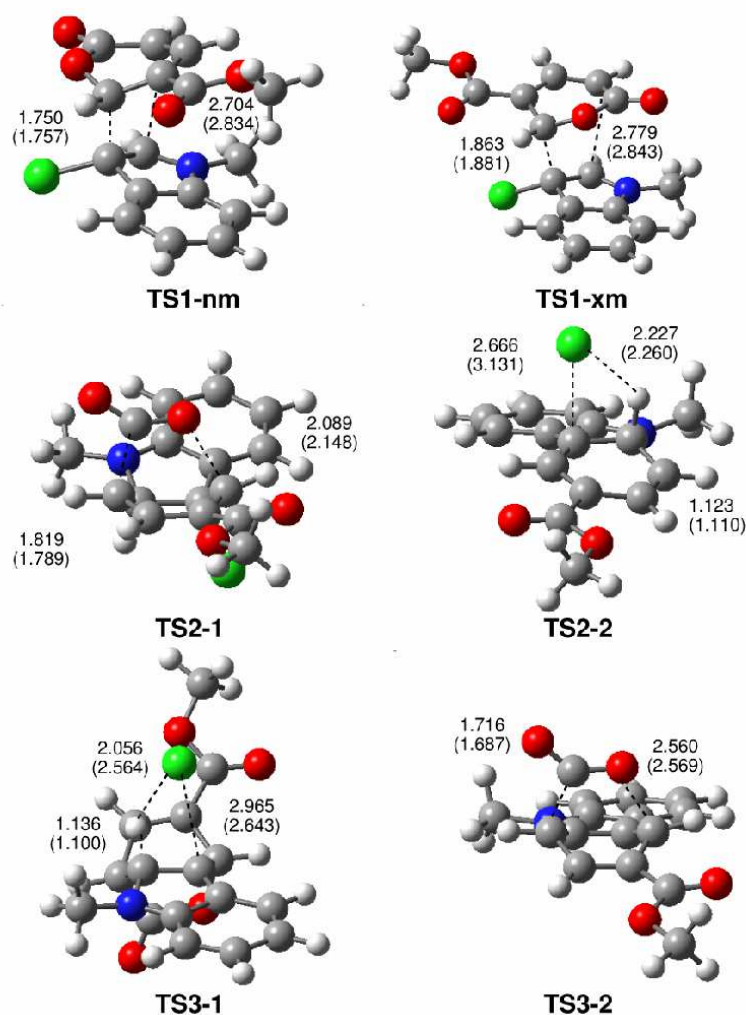


Figure 2. Gas phase optimised transition state geometries involved in the domino reaction between 3-chloroindole **10a** and methyl coumalate **11** including some selected bond lengths in Å. Corresponding values in toluene are given in parentheses.

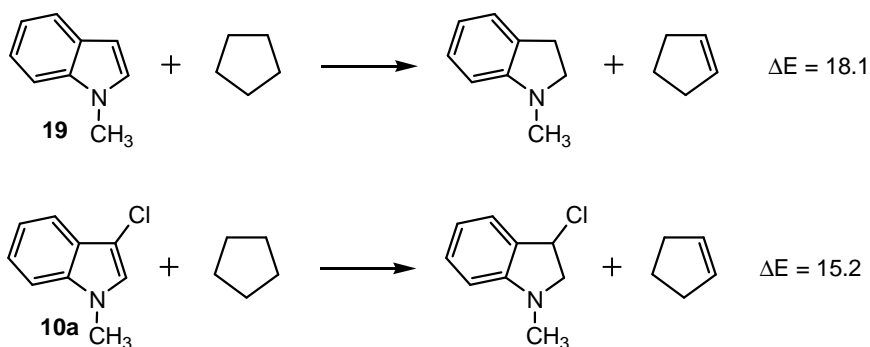
Inclusion of solvent does not produce remarkable changes when gas phase stationary points are re-optimised in toluene. At the TSs involved in the P-DA reaction, the lengths of the C–C forming bonds are slightly longer, indicating that these TSs are slightly more delayed in toluene. In spite of this behaviour, the C3–C4 bond length at the TSs is very short: 1.757 Å at **TS1-nm** and 1.881 Å at **TS1-xm**, indicating that the C–C bond formation has already begun.²⁹ A similar trend is observed in the TSs associated with the extrusion of CO₂, where the TSs in toluene are slightly delayed. A different behaviour is found at the TSs associated with the HCl eliminations along the two competitive channels: while at **TS2-2** the Cl–C breaking bond is more advanced in toluene, it is more delayed at **TS1-3**.

The polar nature of the P-DA reaction between 3-chloroindole **10a** and methyl coumalate **11** was analysed by computing the GEDT along the cycloaddition. The natural atomic charges at **TS1-nm** and **TS1-xm**, obtained through a natural population analysis (NPA), are shared between the indole and the coumalate frameworks. The GEDT that fluxes from the indole framework to the coumalate framework along these DA reactions is 0.34e at **TS1-nm**, and 0.35e at **TS1-xm**. These high values confirm the high polar character of this P-DA reaction. This GEDT is higher than that calculated at the *exo* TS associated with the P-DA reaction between bicyclic enone **7** and *N*-methyl pyrrole **6**, 0.30e (see Scheme 2).¹⁰

Why are P-DA reactions involving indole unfavourable? The polar character of DA reactions is a favourable factor determining the feasibility of the reaction.³ However, this favourable factor may be influenced by other electronic factors such as the aromatic character of the reagents involved in the cycloaddition.¹⁰ Thus, for the P-DA reactions of nucleophilic Cp **4**, and FAHCs furan **5** and pyrrole **6** with bicyclic enone **7** shown in Scheme 2, the increase of activation energies, 19.9 (**4**), 26.2 (**5**), and 29.9 (**6**) kcal/mol, follows the same trend as their GEDTs, 0.16e (**4**), 0.21e (**5**) and 0.30e (**6**), an opposite trend to that found in P-DA reactions involving non-aromatic compounds. The unfavourable activation energies found in the P-DA reactions of **5** and **6** have been associated with the loss of the aromatic character of these FAHCs along the reaction.

This behaviour was supported by studying the aromatic character of these FAHCs through a series of isodesmic reactions.¹⁰

In order to assert the role of the aromatic character of 3-chloroindole **10a** in the high activation energy found in its P-DA reaction toward methyl coumalate **11**, the isodesmic reactions³⁰ shown in Scheme 4, were studied.

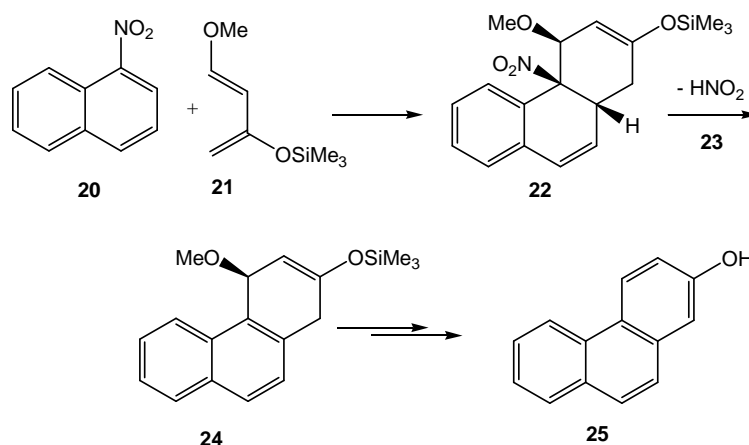


Scheme 4. MPWB1K/6-311G(d,p) isodesmic reactions used to estimate the aromatic character of *N*-methyl-3-chloroindole **10a** (*N*-methyl-indole **19** was used as reference). ΔE values are in kcal/mol.

The relative energies of the isodesmic reactions given in Scheme 7 indicate that the presence of the chlorine atom in 3-chloroindole **10a** produces a slight decrease of the aromatic stabilisation of *N*-methyl indole. When these energies are compared to those associated with the corresponding isodesmic reactions of Cp **4**, 3.0 kcal/mol, and *N*-methyl pyrrole **6**, 29.9 kcal/mol,¹⁰ it can be observed that the FAHC framework of indoles has a lower aromatic character than that in pyrrole **6**, but its electronic stabilisation is higher than that observed in the conjugated 1,3-diene system present in Cp **4**. If we consider the very advanced character of the TSs associated with the P-DA reaction between 3-chloroindole **10a** and methyl coumalate **11**, at this point of the reaction the aromatic character of indole has been lost, requiring a great deal of energy. This behaviour accounts for the unfavourable activation energies found in these DA reactions with a high polar character. In addition, while most P-DA reactions involving 1,3-butadienes are exothermic by more than 20 kcal/mol,³ this P-DA reaction is exothermic by only 11 kcal/mol. After including the unfavourable entropy term associated with these bimolecular processes, most P-DA reactions remain exergonic,

whereas those involving aromatic compounds become endergonic, thus being kinetically and thermodynamically unfavourable.¹⁰

A similar behaviour was found in the P-DA reaction between 1-nitro-naphthalene **20** and the Danishefsky diene **21**, in which the formation of the formal [2+4] CA **22** was kinetically ($\Delta G^\ddagger = 39.3$ kcal/mol) and thermodynamically ($\Delta G_r = 22.2$ kcal/mol) very unfavourable due to the aromatic character of naphthalene (see Scheme 5).³¹ However, the strong exergonic character of the subsequent extrusion of nitrous acid **23** yielding intermediate **24**, -17.1 kcal/mol, favours the irreversible formation of the final phenanthrene derivative **25**.



Scheme 5

Again, the presence of an easily removable nitro group, NO₂, in the aromatic compound is the driving force of these domino reactions initialised by an unfavourable P-DA reaction.

ii) *ELF topological analysis of the P-DA reaction between 3-chloroindole **10a** and methyl coumalate **11**.*

A great deal of work has emphasised that the ELF topological analysis of the bonding changes along a reaction path is a powerful tool to establish the molecular mechanism of a reaction.¹⁵ After an analysis of the electron density, ELF provides basins which are the domains in which the probability of finding an electron pair is maximal. The basins are classified as core and valence basins. The latter are characterised by the synaptic order, *i.e.* the number of atomic valence shells in which

they participate.³² Thus, there are monosynaptic, disynaptic, trisynaptic basins and so on. Monosynaptic basins, labelled $V(A)$, correspond to lone pairs or non-bonding regions, while disynaptic basins, labelled $V(A,B)$, connect the core of two nuclei A and B and, thus, correspond to a bonding region between A and B. This description recovers the Lewis bonding model, providing a very suggestive graphical representation of the molecular system.

A great deal of work characterising the mechanisms of significant organic reactions involving the formation of new C–C single bonds has shown that it begins in the short C–C distance range of 1.9 - 2.0 Å by merging two monosynaptic basins, $V(C_x)$ and $V(C_y)$, into a new disynaptic basin $V(C_x,C_y)$ associated with the formation of the new C_x–C_y single bond.²⁹ The C_x and C_y carbons characterised by the presence of the monosynaptic basins, $V(C_x)$ and $V(C_y)$, have been called *pseudoradical* centers.³³

In order to understand the molecular mechanism of the P-DA reaction between 3-chloroindole **10a** and methyl coumalate **11**, an ELF topological analysis of the MPWB1K/6-311G(d,p) wavefunctions of some relevant points along the IRC profile associated with **TS1-xm** was performed. Details of the ELF topological analysis are given in the Supporting Information.

Some appealing conclusions can be drawn from this ELF topological analysis:

- i) ELF topological analysis along the one-step P-DA reaction between 3-chloroindole **10a** and methyl coumalate **11** indicates that the bonding changes take place at least in 15 differentiated phases; each one of these phases corresponds to a bonding change with respect to the previous Lewis structure. Consequently, the bonding changes in this P-DA reaction are non-concerted;
- ii) as in the most of organic reactions, formation of the first C3–C4 single bond takes place at a distance of 1.927 Å, through the coupling of two *pseudoradical* centers created at the most nucleophilic center of 3-chloroindole **10a**, the C3 carbon, and the most electrophilic center of methyl coumalate **11**, the C4 carbon.²⁹ These relevant centers are clearly characterised when the electrophilic and nucleophilic Parr functions²⁸ are analysed at the ground state of the separated reagents (see later);

iii) at point **P8**, the maximum GEDT in this P-DA reaction, 0.45e, is reached.

Beyond this point, there is a GEDT decrease as a consequence of a retrodonation process associated with the formation of the second C–C single bond;

iv) formation of the second C2–C7 single bond takes place at a C–C distance of 2.019 Å at the last phase of the reaction. At this stage, the C3–C4 single bond, represented by the V(C3,C4) disynaptic basin with a population of 1.92e, is practically completed, in clear agreement with a *two-stage one-step* mechanism.¹¹

Interestingly, ELF topological analysis of **TS1-xm** indicates that while formation of the first C3–C4 single bond has already begun, with a C3–C4 length of 1.863 Å and a population of 1.34e, formation of the second C2–C7 single bond with a C2 and C7 length of 2.779 Å is very delayed (See the presence of the V(C2,C3) attractor and the absence of any V(C2) and V(C7) attractors in **TS1-xm** in Figure 3). Valence basin populations *N* of **TS1-xm** are given in Table S1 of the Supporting Information. Note that in most of the TSs associated with P-DA reactions showing a C–C distance larger than 2.1 Å,³ the formation of the first C–C single bond has not started. This behaviour of **TS1-xm**, showing a very high asynchronicity in the formation of the two C–C single bonds, clearly shows the non-concerted nature of this P-DA reaction. On the other hand, the very advanced sp³ character of the C3 carbon of indole **10** at **TS1-xm** suggests the loss of the aromatic character of the five-membered heterocyclic ring of indole, and accounts for the high activation energy associated with the formation of this TS.

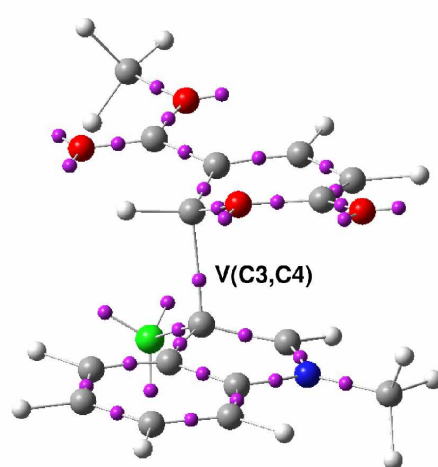


Figure 3. ELF attractor positions in **TS1-xm**. While the presence of the $V(C3,C4)$ attractor indicates that the formation of the C3–C4 single bond with a population of 1.34e has begun, the absence of the $V(C2)$ and $V(C7)$ attractors indicates that formation of the C2–C7 single bond is very delayed, in clear agreement with a *two-stage one-step* mechanism.¹¹

The bonding changes associated with the formation of the first C3–C4 single bond are similar to those associated with the formation of C3–C4 single bond in the Friedel-Crafts reaction between *N*-methyl indole **19** and an electrophilically activated nitroolefin.³⁴ This similarity in the C–C bond formation found in these two different organic reactions, a DA reaction and an AES reaction, allows establishing that P-DA reactions begin through a nucleophilic/electrophilic two-center interaction as in most polar organic reactions. Formation of the different products occurs at the second part of the reaction when the first C–C single bond is practically formed. These reactions can take place *via* a *one-step two-stage* mechanism as in most P-DA reactions, or *via* a stepwise mechanism with formation of a zwitterionic intermediate as in the aforementioned Friedel-Crafts reaction. Regardless of the *one-step* or stepwise nature of the reaction mechanism, the bonding changes at the first stage of the one step mechanism and those at the first step of the stepwise one are very similar. This quantum chemical topological similarity of both mechanisms supports Domingo's proposal that DA reactions are not a special type of organic reaction.²⁹

iii) Analysis of the global and local reactivity indices of the reagents involved in the P-DA reaction.

Finally, the P-DA reaction between 3-chloroindole **10a** and methyl coumalate **11** were analysed using the reactivity indices defined within conceptual DFT.⁶ The values of global descriptors, namely, electronic chemical potential μ , chemical hardness η , global electrophilicity ω , and global nucleophilicity N indices for the reagents involved in the studied P-DA reaction are given in Table 3.

Table 3. MPWB1K/6-311G(d,p) electronic chemical potential μ , chemical hardness η , global electrophilicity ω , and global nucleophilicity N indices, in eV, of 3-chloroindole **10a** and methyl coumalate **11**.

	μ	η	ω	N
11	-4.59	6.77	1.55	2.43
10a	-3.14	6.73	0.73	3.89

The electronic chemical potential μ of 3-chloroindole **10a**, -3.14 eV, is higher than that of methyl coumalate **11**, -4.59 eV. Consequently, along this P-DA reaction the GEDT will take place from 3-chloroindole **10a** to methyl coumalate **11**, in clear agreement with the GEDT computed at the TSs associated with this P-DA reaction.

The electrophilicity ω index of methyl coumalate **11** is 1.55 eV, being classified as a moderate electrophile. On the other hand, the nucleophilicity N index of **11** is 2.43 eV, being classified also as a moderate nucleophile. The electrophilicity ω index of 3-chloroindole **10a** is 0.73 eV, being classified as a marginal electrophile. Consequently, indole **10a** will not participate as an electrophile in polar reactions. The nucleophilicity N index of **10a** is 3.89 eV, being classified as a strong nucleophile. The nucleophilicity N index of **10a** is similar to that of *N*-methyl pyrrole **6**, 3.70 eV. However, the higher aromatic character of the latter makes it less reactive. Consequently, the analysis of the global reactivity indices indicates that along this P-DA reaction, methyl coumalate **11** will participate as the electrophile, while 3-chloroindole **10a** will do so as the nucleophile.

Along a polar reaction involving the participation of asymmetric reagents, the most favourable reactive channel is that involving the initial two-center interaction between the most electrophilic center of the electrophile and the most nucleophilic center of the nucleophile.³⁵ Recently, we have proposed the electrophilic P_k^+ and nucleophilic P_k^- Parr functions derived from the excess of spin electron density reached *via* the GEDT process from the nucleophile to the electrophile as powerful tools in the study of the local reactivity in polar processes.²⁸ Accordingly, the electrophilic P_k^+ Parr functions for methyl coumalate **11** and nucleophilic P_k^- Parr functions for 3-chloroindole **10a** are analysed (see Figure 4).

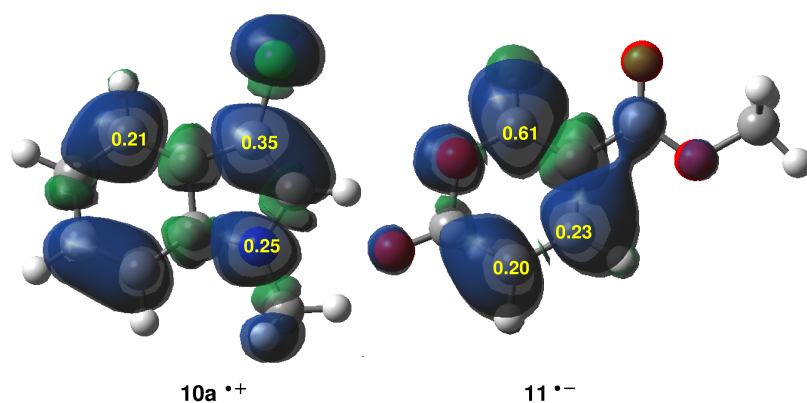


Figure 4. MPWB1K/6-311G(d,p) maps of the ASD of radical cation **10a** \bullet^+ and nucleophilic P_k^- Parr functions of 3-chloroindole **10a**, and ASD of radical anion **11** \bullet^- and electrophilic P_k^+ Parr functions of methyl coumalate **11**.

Analysis of the electrophilic P_k^+ Parr functions in methyl coumalate **11** indicates that the C4 carbon is the most electrophilic center of this molecule, $P_k^+ = 0.61$. The C4 carbon, which corresponds to the β and the δ conjugated positions with respect to the carboxylate groups present at the C5 and the C7 carbons, is three times more activated than the C6, $P_k^+ = 0.23$, and the C7, $P_k^+ = 0.20$, carbons. On the other hand, analysis of the nucleophilic P_k^- Parr functions in 3-chloroindole **10a** indicates that the C3 carbon is the most nucleophilic center of this molecule, $P_k^- = 0.35$, followed by the N1 nitrogen atom, $P_k^- = 0.25$. Note that the C2 carbon of **11** does not present any nucleophilic activation. In addition, it is worth mentioning that the N1–C2–C3 framework of indole

10a constitutes an aza-allyl system. Consequently, the most favourable two center nucleophilic/electrophilic interaction along the nucleophilic attack of 3-chloroindole **10a** on methyl coumalate **11** will take place along the approach of the C2 carbon of **10a** and the C4 carbon of **11**. Interestingly, this pattern of local nucleophilic activation is opposite that found in *N*-methyl pyrrole **6**, in which the C2 and C5 carbons are the most nucleophilic centers of this FAHC molecule.¹⁰

Finally, the larger electrophilic activation of the C4 carbon of methyl coumalate **11** than that in the C7 one accounts for the complete regioselectivity expected in the P-DA reaction between **10a** and **11**. Note that carbazole **12a** is the only isomeric product obtained along this domino reaction.

Conclusions

The molecular mechanism of the domino reaction between *N*-methyl-3-chloroindole **10a** and methyl coumalate **11** yielding carbazole **12a** has been studied using DFT methods at the MPWB1K/6-311G(d,p) level in toluene. Formation of carbazole **12a** takes place through a domino process that comprises three consecutive reactions: *i*) a P-DA reaction between 3-chloroindole **10a** and methyl coumalate **11** to yield the stereoisomeric CAs **13** and **14**; *ii*) an elimination of hydrochloric acid from these CAs affording intermediate **18** and its corresponding stereoisomer; and finally *iii*) an extrusion of CO₂ in these intermediates yielding carbazole **12a**.

The P-DA reaction between **10a** and **11** is completely regioselective and slightly *exo* selective, but both *endo* and *exo* CAs experience HCl and CO₂ eliminations yielding the same carbazole **12a**. In spite of the high polar character of this P-DA reaction, the GEDT in this polar reaction is 0.35e, it has a high activation enthalpy of 21.8 kcal/mol as a consequence of the aromatic character of indole **10a**, which is lost along the formation of the first C-C single bond. Thermodynamic calculations suggest that the initial HCl elimination in the [2+4] CAs is kinetically favoured over the extrusion of CO₂. The large energy difference between the TSs involved in these initial elimination reactions, 7.8 kcal/mol, makes it possible to rule out the initial loss of CO₂ proposed by experimentalists.¹²

Due to the aromatic character of *N*-methyl-3-chloroindole **10a**, the loss of aromatic stabilisation along the P-DA reaction makes it kinetically and

thermodynamically very unfavourable. However, the lower activation enthalpies associated with the HCl and CO₂ elimination together with the strong exergonic character of the CO₂ extrusion make the overall domino process irreversible. Consequently, the adequate substitution in *N*-methyl-3-chloroindole **10a** and methyl coumalate **11** favouring the irreversible loss of HCl and CO₂ enables the unfavourable P-DA reaction.

ELF topological analysis of the bonding changes along the *exo* stereoisomeric path of the P-DA reaction between **10a** and **11** enables the characterisation of at least 15 distinguishable phases. The C3–C4 and C2–C7 single bonds are formed through the coupling of two *pseudoradical* centers at **P7**, $d(\text{C3–C4}) = 1.927 \text{ \AA}$ and $d(\text{C2–C7}) = 2.800 \text{ \AA}$, and **P15**, $d(\text{C3–C4}) = 1.566 \text{ \AA}$ and $d(\text{C2–C7}) = 2.019 \text{ \AA}$, with an initial population of 1.19e and 1.20e, respectively. This topological analysis supports the *one-step two-stage* mechanism easily characterised by a geometrical analysis of the changes in C–C lengths along cycloadditions. Interestingly, the *exo* **TS1-xo** associated with this P-DA reaction is found in the phase characterised by **P8**, *i.e.* at **TS1-xo** the C3–C4 single bond formation has already started, while the distance between the C2 and C7 carbons is very high, 2.779 Å. This behaviour of **TS1-xo** clearly shows the non-concerted nature of this P-DA reaction.

An analysis of the DFT reactivity indices in reagents indicates that the strong nucleophilic character of 3-chloroindole **10a** and the moderate electrophilic character of methyl coumalate **11** are responsible for the high polar character of this DA reaction.

Finally, analysis of the nucleophilic P_k^- Parr functions in 3-chloroindole **10a** and the electrophilic P_k^+ Parr functions in methyl coumalate **11** offers an explanation of the total regioselectivity found in this P-DA reaction. While the C3 carbon of 3-chloroindole **10a** is the most nucleophilic center of this molecule, the C4 carbon of methyl coumalate **11** is three times more electrophilically activated than the C7 carbon. Consequently, the most favourable nucleophilic/electrophilic two center interactions along this P-DA reaction will take place between the C3 carbon of **10a** and the C4 carbon of **11**, in complete agreement with the fact that carbazole **12a** is formed as the only product of this reaction.

Supporting Information. ELF topological analysis of the P-DA reaction between 3-chloroindole **10a** and methyl coumalate **11**. MPWB1K/6-311G(d,p) gas phase total and relative, enthalpies, entropies, and Gibbs free energies computed at 200 °C and 1 atm in toluene, and cartesian coordinates of the optimised structures in toluene, involved in the P-DA reaction between 3-chloroindole **10a** and methyl coumalate **11**.

Acknowledgements

L. R. D. thanks to Ministerio de Ciencia e Innovación of the Spanish Government, project CTQ2013-45646-P, for financial support.

References

- 1 (a) Carruthers, W. *Some Modern Methods of Organic Synthesis*; second ed.; Cambridge University Press: Cambridge, 1978. (b) Carruthers, W. *Cycloaddition Reactions in Organic Synthesis*; Pergamon: Oxford, 1990.
- 2 Rowley, D.; Steiner, H. *Discussions of the Faraday Society* **1951**, 198-213.
- 3 Domingo, L. R.; Sáez, J. A. *Org. Biomol. Chem.* **2009**, *7*, 3576-3583.
- 4 Parr, R. G.; Von Szentpaly, L.; Liu, S. B. *J. Am. Chem. Soc.* **1999**, *121*, 1922-1924.
- 5 Domingo, L. R.; Chamorro, E.; Pérez, P. *J. Org. Chem.* **2008**, *73*, 4615-4624.
- 6 (a) Geerlings, P.; De Proft, F.; Langenaeker, W. *Chem. Rev.* **2003**, *103*, 1793-1873. (b) Ess, D. H.; Jones, G. O.; Houk, K. N. *Adv. Synth. Catal.* **2006**, *348*, 2337-2361.
- 7 (a) Della Rosa, C.; Kneeteman, M. N.; Mancini, P. M. E. *Tetrahedron Letters* **2005**, *46*, 8711-8714. (b) Brasca, R.; Kneeteman, M. N.; Mancini, P. M. E.; Fabián, W. M. F. *J. Mol. Struct. (THEOCHEM)* **2009**, *911*, 124-131. (c) Della Rosa, C.; Ormachea, C.; Kneeteman, M. N.; Adam, C.; Mancini, P. M. E. *Tetrahedron Letters* **2011**, *52*, 6754-6757.
- 8 Della Rosa, C. D.; Sánchez, J. P.; Kneeteman, M. N.; Mancini, P. M. E. *Tetrahedron Letters* **2011**, *52*, 2316-2319.

- 9 (a) Domingo, L.R.; Jones, R.A.; Picher, M.T.; Sepulveda-Arques, J. *Tetrahedron* **1995**, *51*, 8739-8748. (b) Jursic, B. S. *Can. J. Chem.* **1996**, *74*, 114-120. (c) Jursic, B. S. *J. Mol. Struct. (THEOCHEM)* **1998**, *454*, 277-286. (d) Domingo, L. R.; Picher, M. T.; Zaragoza, R. J. *J. Org. Chem.* **1998**, *63*, 9183-9189. (e) Domingo, L. R.; Picher, M. T.; Aurell, M. J. *J. Phys. Chem. A* **1999**, *103*, 11425-11430. (f) Vijaya, R.; Dinadayalane, T. C.; Sastry, G. N. *J. Mol. Struct. (THEOCHEM)* **2002**, *589*, 291-299.
- 10 Domingo, L. R.; Pérez, P.; Ortega, D. E. *J. Org. Chem.* **2013**, *78*, 2462-2471.
- 11 Domingo, L. R.; Sáez, J. A.; Zaragoza, R. J.; Arnó, M. *J. Org. Chem.* **2008**, *73*, 8791-8799.
- 12 Guney, T.; Lee, J. J.; Kraus, G. A. *Org. Lett.* **2014**, *16*, 1124-1127.
- 13 Savin, A.; Becke, A. D.; Flad, J.; Nesper, R.; Preuss, H.; von Schnering, H. G. *Angew. Chem. Int. Ed.* **1991**, *30*, 409-412. (b) Silvi, B.; Savin, A. *Nature* **1994**, *371*, 683. (c) Savin, A.; Silvi, B.; Colonna, F. *Can. J. Chem.* **1996**, *74*, 1088-1096. (d) Savin, A.; Nesper, R.; Wengert, S.; Fassler, T. F. *Angew. Chem., Int. Ed. Engl.* **1997**, *36*, 1809-1832.
- 14 Fukui, K. *J. Phys. Chem.* **1970**, *74*, 4161-4163.
- 15 (a) Polo, V.; Andrés, J.; Berski, S.; Domingo, L. R.; Silvi, B. *J. Phys. Chem. A* **2008**, *112*, 7128-7136. (b) Andrés, J.; Berski, S.; Domingo, L. R.; Polo, V.; Silvi, B. *Curr. Org. Chem.* **2011**, *15*, 3566-3575. (c) Andrés, J.; Berski, S.; Domingo, L. R.; González-Navarrete, P. *J. Comput. Chem.* **2012**, *33*, 748-756.
- 16 Zhao, Y.; Truhlar, D. G. *J. Phys. Chem. A* **2004**, *108*, 6908-6918.
- 17 Hehre, W. J.; Radom, L.; Schleyer, P. v. R.; Pople, J. A. *Ab initio Molecular Orbital Theory*; Wiley: New York, 1986.
- 18 (a) Schlegel, H. B. *J. Comput. Chem.* **1982**, *3*, 214-218. (b) Schlegel, H. B. *Modern Electronic Structure Theory*; Yarkony, D. R., Ed.; World Scientific Publishing: Singapore, 1994.
- 19 (a) González, C.; Schlegel, H. B. *J. Phys. Chem.* **1990**, *94*, 5523-5527. (b) González, C.; Schlegel, H. B. *J. Chem. Phys.* **1991**, *95*, 5853-5860.
- 20 (a) Tomasi, J.; Persico, M. *Chem. Rev.* **1994**, *94*, 2027-2033. (b) Simkin, B.Y.; Sheikhet, I. *Quantum Chemical and Statistical Theory of Solutions-A Computational Approach*; Ellis Horwood: London, 1995.

- 21 (a) Cancès, E.; Mennucci, B.; Tomasi, J. *J. Chem. Phys.* **1997**, *107*, 3032-3041.
(b) Cossi, M.; Barone, V.; Cammi, R.; Tomasi, J. *Chem. Phys. Lett.* **1996**, *255*, 327-335. (c) Barone, V.; Cossi, M.; Tomasi, J. *J. Comput. Chem.* **1998**, *19*, 404-417.
- 22 (a) Reed, A. E.; Weinstock, R. B.; Weinhold, F. *J. Chem. Phys.* **1985**, *83*, 735-746. (b) Reed, A. E.; Curtiss, L. A.; Weinhold, F. *Chem. Rev.* **1988**, *88*, 899-926.
- 23 Becke, A. D.; Edgecombe, K. E. *J. Chem. Phys.*, **1990**, *92*, 5397-5403.
- 24 Noury, S.; Krokidis, X.; Fuster, F.; Silvi, B. *Chem.*, **1999**, *23*, 597-604.
- 25 Frisch, M. J.; *Gaussian 09*; Gaussian, Inc., Wallingford CT, **2009**.
- 26 (a) Parr, R. G.; Pearson, R. G. *J. Am. Chem. Soc.* **1983**, *105*, 7512-7516. (b) Parr, R. G.; Yang, W. *Density Functional Theory of Atoms and Molecules*; Oxford University Press: New York, 1989.
- 27 Kohn, W.; Sham, L. J. *Phys. Rev.* **1965**, *140*, 1133-1138.
- 28 Domingo, L. R. Pérez, P.; Sáez, J. A. *RSC Adv.*, **2013**, *3*, 1486-1494.
- 29 Domingo, L. R. *RSC Adv.* **2014**, *4*, 32415-32428.
- 30 Carey, F. A.; Sundberg, R. J. *Advanced Organic Chemistry. Part A: Structure and Mechanisms*; Springer: New York, 2000.
- 31 Domingo, L.R., Aurell, M.J., Kneeteman, M.N.; Mancini, P. M. *J. Mol. Struct. (THEOCHEM)* **2008**, *853*, 68-76
- 32 Silvi, B. *J. Mol. Struct.* **2002**, *614*, 3-10.
- 33 Domingo, L. R.; Chamorro, E.; Pérez, P. *Lett. Org. Chem.* **2010**, *7*, 432-439.
- 34 Domingo, L. R.; Pérez, P.; Sáez, J. A. *RSC Adv.* **2013**, *3*, 7520-7528.
- 35 Domingo, L. R.; Pérez, P.; Sáez, J. A. *Tetrahedron* **2013**, *69*, 107-114.